

## The Iron Distribution in Rhodonite

BRUCE L. DICKSON

*Department of Solid State Physics, Research School of Physical Sciences,  
The Australian National University, Canberra, A.C.T. 2600 Australia*

### Abstract

The Mössbauer spectra of four rhodonite samples have been obtained at 298 and 77 K. All the iron is in the ferrous state and is distributed among the five cation sites in rhodonite. Most of the iron is in the octahedral coordinated  $M_1$ ,  $M_2$ , and  $M_3$  sites, but as these sites could not be individually distinguished in the spectra, the relative site populations were not obtained. The  $\text{Fe}^{2+}$  ions show a small preference for the near five-coordinate  $M_4$  site, and little iron enters the seven-coordinate  $M_5$  site.

### Introduction

A number of optical studies have been made on the chain silicate rhodonite,  $(\text{Mn,Fe,Ca,Mg})\text{SiO}_3$ , principally with manganese-rich samples (*e.g.*, Lakshman and Reddy, 1973; Manning, 1968). Some studies have included spectra of iron-rich ( $\sim 25$  percent  $\text{FeSiO}_3$ ) rhodonite (Keester and White, 1968), but to analyze these spectra the distribution of the iron amongst the metal cation sites in rhodonite must be known.

Rhodonite has the structure of a triclinic pyroxenoid with space group  $P\bar{1}$  (Peacor and Niizeki, 1963). The structure contains chains of  $[\text{SiO}_4]$  tetrahedra with a repeat unit of five tetrahedra. Layers of chains alternate between planes of close packed oxygen ions with layers of coordinated cations. There are five equally populated cation positions in rhodonite; four designated  $M_1$ ,  $M_2$ ,  $M_3$ , and  $M_4$  give sixfold coordination and the fifth,  $M_5$ , gives an irregular sevenfold coordination. Site  $M_4$  has one elongated  $M$ -O bond, making this site nearer five-coordination. The metal coordination polyhedra as determined for the low iron rhodonite are illustrated in Figure 1. Three types of oxygen ions occur in the rhodonite structure; type *A* are coordinated to 2 Si and one  $M$  ion, type *B* are coordinated to one Si and 3  $M$  ions, and type *C* to one Si and 2  $M$  ions. The three types of oxygen ions will have different effective charges in the order  $A < B < C$ . This is reflected in the  $M$ -O bond lengths with *A* type  $M$ -O bonds being on average the longest and *C* type the shortest.

On the basis of an electron density difference synthesis and the difference in sizes of the five sites, Peacor and Niizeki (1963) located all the calcium ions in the  $M_5$  site, the iron and magnesium ions in the  $M_4$  site, and distributed the manganese ions so as to give all five sites equal population. However, the restriction of the iron to one site while the manganese ions occurred in all five sites appeared unreasonable, and a preliminary Mössbauer spectrum of a rhodonite sample showed that the iron was distributed amongst several sites. Consequently, a number of rhodonite samples were examined by Mössbauer spectroscopy to determine the distribution of iron among the five sites and the effect of composition on this distribution.

### Experimental

Four rhodonite samples were examined in this study though the iron distribution in the iron-rich sample, labelled A, for which polarized absorption spectra have been obtained (Marshall and Runciman, to be published), was of major interest. The compositions of the samples A, C, and D were obtained by electron microprobe analysis. The results of the analyses and details of the sources of the samples are given in Table 1. Iron and manganese are expressed as FeO and MnO, respectively, and no independent analysis was made of the ferric iron content.

Mössbauer spectra of each sample were taken on a constant acceleration spectrometer using a 50-mC  $^{57}\text{Co}$  source in palladium matrix. The spectra were

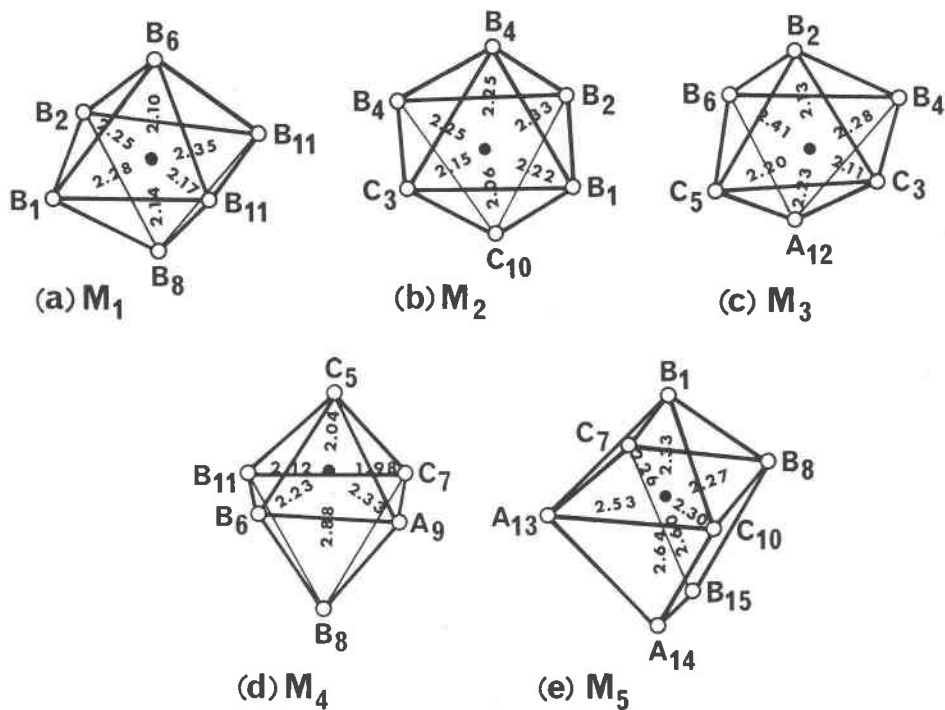


FIG. 1. Projections of the oxygen coordination polyhedra about the five cation positions in rhodonite, derived from the structure determination of Peacor and Niizeki (1963). Metal-oxygen distances are indicated. The letters A, B, and C indicate the oxygen ion type, as described in the text.

accumulated in a PDP 11/10 minicomputer which also produced the velocity reference waveform (Window, Dickson, Routcliffe and Srivastava, 1974). Generally, 256 channel spectra were obtained but, for sample A, 512 channels were used to obtain higher resolution. Velocity calibration was made against the spectrum of iron foil using the data of Violet and Pipcorn (1971) and isomer shifts (IS) are reported relative to iron.

The rhodonite samples were ground to a fine powder and packed between tape in a thin paper disc. No evidence of preferred orientation was seen in the spectra. A sample thickness of approximately 0.1 gm/cm<sup>2</sup> was used.

The spectra were analyzed using the least squares method to fit Lorentzian shaped peaks. The weighted sum of the squares of the difference between each channel count and the value of the fitted function at that channel ( $\chi^2$ ) is minimized. Various constraints were placed on the parameters fitted to the data to enable the value of  $\chi^2$  to converge. These are discussed later. The statistical acceptable values of  $\chi^2$  lie between the 1 and 99 percent points of the  $\chi^2$  distribution; that is, in the range  $\nu + 2.2 \pm 3.3\sqrt{\nu}$ ,

where  $\nu$  is the number of degrees of freedom (Bancroft, Burns, and Stone, 1968). However, with complex spectra, assumptions such as that of Lorentzian lineshape can give higher values of  $\chi^2$  with what may be judged as a reasonable model to fit to the data. Thus, in deciding on the "goodness of fit,"  $\chi^2$  must be taken as only one of several factors, such as the smoothness of a plot of the residuals, the size of the standard deviations in each parameter, and how well the parameters compare to those obtained with other, similar samples.

The validity of fitting peaks broader than natural width as Lorentzian shaped must be considered. The causes of peak broadening will generally lead to the experimental peak shape being the result of a Gaussian distribution of Lorentzians. The resulting profile cannot be easily represented for use in fitting programs, and linear combinations of Lorentzian and Gaussian terms have been used instead (Dowty and Lindsley, 1973; Evans and Black, 1970). In this case, it was felt the extra parameter introduced for each doublet fitted (the linear combination term) would not be justified, and pure Lorentzian-shaped peaks were used.

TABLE 1. Compositions and Sources of Rhodonites

	A	B	C	D
SiO <sub>2</sub>	46.71	45.30	46.03	45.61
MnO	31.64	33.43	44.75	46.04
FeO	12.46	12.13	2.14	1.57
CaO	9.04	8.62	7.14	6.26
MgO	0.32	0.54	0.49	0.47
Total	100.17	100.02	100.55	99.95
Metal Ion Present as Atomic Percent				
Mn	56.6	58.4	78.8	81.7
Fe	22.0	20.9	3.7	2.7
Ca	20.4	19.0	15.9	14.1
Mg	1.0	1.6	1.5	1.5

A Single crystal rhodonite, Zinc Corporation Mine, Broken Hill, N.S.W., Australia (further details given in Overton (1968).  
 B Brown crystalline matrix, Broken Hill, N.S.W.  
 C Brown-red mass, Cornwall, England  
 D Violet mass, Devon, England

## Results

The Mössbauer spectra of the four rhodonite samples were obtained at 295 K and 77 K. The samples gave very similar spectra at each temperature. Two representative spectra are shown in Figure 2.

The spectra contain four broad absorption peaks which can be grouped into two doublets nested one inside the other. The asymmetry of the bottom of the outer, more intense peaks shows that these are composed of two or more peaks. Between the higher velocity peaks there is also evidence of another less intense peak. A spectrum of sample A was obtained at 495 K and is shown in Figure 3. This shows a shoulder at  $\approx 1.8$  mm/sec quite clearly. The nine spectra were thus first fitted with four nested doublets, each doublet having independent centers, splittings, widths, and amplitudes.

The fitting procedure converged in each case to an acceptable value of  $\chi^2$ , and the individual position parameters fitted to the four spectra taken at 298 K were the same to within  $\pm 0.003$  mm/sec. Similarly, the four spectra taken at 77 K were fitted with very similar parameters. However, large standard deviations in the width and amplitude parameters were found with all nine spectra, particularly with the two central doublets, indicating a large dependence between the parameters of the doublets.

The spectra were reanalyzed using a five-nested doublet model with the three outer doublets constrained to have the same amplitude and widths. The inner two doublets were fitted as previously. This model was chosen to get a better fit of the most

intense peaks of the spectra, though the same number of variable parameters are fitted as initially. When the data were fitted in this manner, only a small decrease in the value of  $\chi^2$  over the previous model was obtained, but the standard deviations of the various parameters decreased by factors of up to ten. The standard deviations of the parameters of the small inner doublet were still larger than those of the other doublets, but this is understandable as this small peak will be grossly affected by any changes in the positions of the much larger peaks on each side of it.

Attempts to release some of the constraints in the fitted model led to divergence in the  $\chi^2$  value, and the five doublet fit was accepted as the best possible. Examples of the fitted envelopes are shown in Figures 2 and 3. As found before, the doublet center and splitting parameters/fitted to the four spectra at 77 K and at 298 K, respectively, were generally within  $\pm 0.01$  mm/sec, the estimated error in the measurement. The three doublets, III, IV, and V, were fitted with centers that varied by no more than  $\pm 0.005$  mm/sec. The average value was also within a similar error of the centers of the two doublets fitted independently to the same peaks. The positions and widths of the two innermost doublets were also within a similar error of parameters obtained in the first analysis, indicating the two models are basically similar.

The parameters derived from the five-doublet fit to the spectra are given in Table 2. The parameters derived from the doublets III, IV, and V are condensed to the average center, the three quadruple splittings, and the total area of the three doublets (relative to the area of the innermost doublet).

## Discussion

### (a) Site Assignments

The doublets fitted to the room temperature spectra have isomer shifts (IS) typical of those found for Fe<sup>2+</sup> ions in coordination with six oxygen ligands in silicate minerals (Bancroft, Maddock, and Burns, 1967). There is no clear evidence of any ferric ions being present in any of the four samples, though a plot of the residuals from the fit to the spectrum of sample A did indicate that the area under the lower velocity peaks was approximately 0.3 percent larger than under the higher velocity peaks. This resulted in slightly greater  $\chi^2$  value for the fit to this particular sample. This is

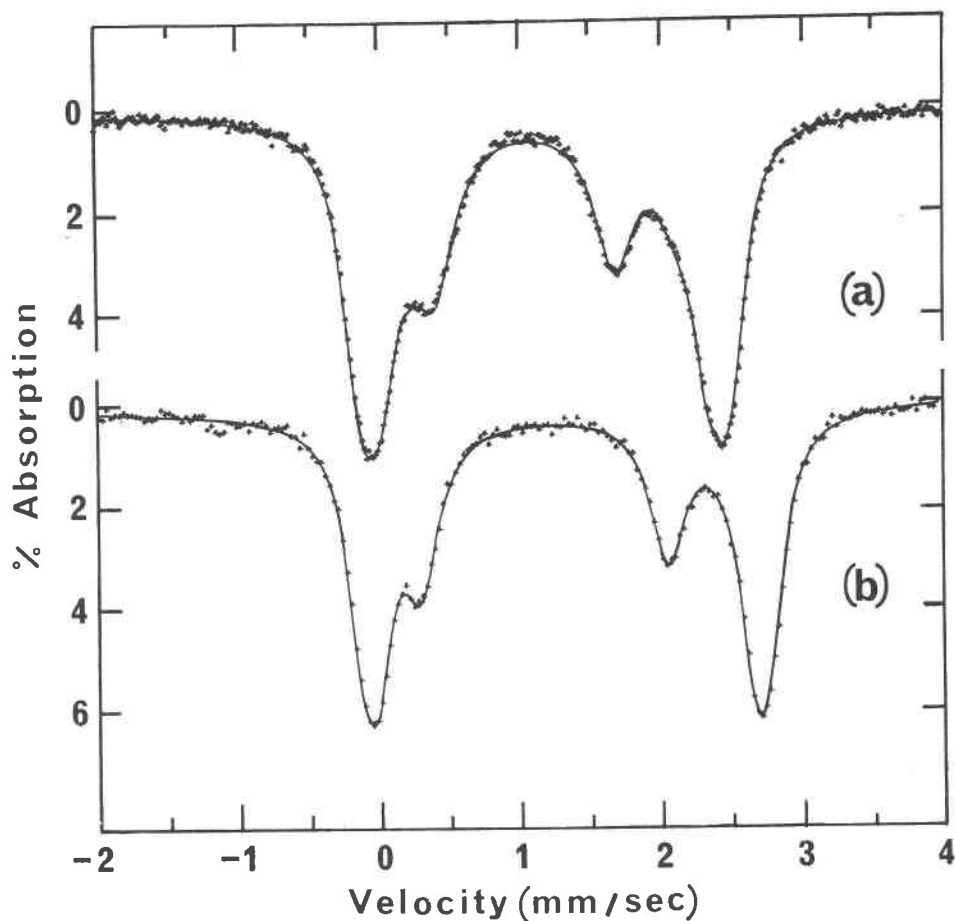


FIG. 2. (a) The Mössbauer spectrum of sample A, taken at 295 K and (b) of sample B taken at 77 K. The solid curves are obtained from fitting five doublets to the data.

possibly due to a trace of  $\text{Fe}^{3+}$  ions, though the amount is at the limit of detection.

The spectra show that the ferrous ions are distributed among the various cation sites and that a similar distribution is found in different rhodonite samples. Doublet I, the innermost, can be assigned to  $\text{Fe}^{2+}$  ions in the  $M_4$  site, as this site has an effective five coordination and is expected to have a smaller IS than a sixfold coordinated ion, assuming the general trend of decreasing IS with decreasing coordination number as seen in other silicate minerals (Bancroft, Maddock, and Burns, 1967). For example, in partially hydrated zeolites where  $\text{Fe}^{2+}$  ions can be found coordinated to three lattice oxygen ions and two water molecules (Dickson and Rees, to be published), IS values are around 1.15 mm/sec. When a third water molecule was attached, the IS increased by approximately 0.1 mm/sec. The IS difference between doublet I and the other four

doublets fitted to the spectra (which will be due to  $\text{Fe}^{2+}$  ions in the sites with higher coordination numbers) is of a similar magnitude. The small quadrupole splitting (QS) of doublet I is also expected if the iron is in the  $M_4$  site, as this site can be regarded as an octahedron with one axial ligand drawn away. This will give a sizeable lattice contribution to the electric field gradient (e.f.g.) at the  $\text{Fe}^{2+}$  nucleus, which is generally of opposite sign to the valence contribution (Ingalls, 1964). Quantitative estimates of the actual QS contributions are difficult to make, but the  $M_4$  site can be considered somewhere between octahedral geometry, where the lattice e.f.g. is near zero and the QS at room temperature is around 3.5 mm/sec, and square planar geometry, where the lattice and valence contributions to the e.f.g. almost cancel and the QS is very small (0.51 mm/sec) (Clark, Bancroft, and Stone, 1967).

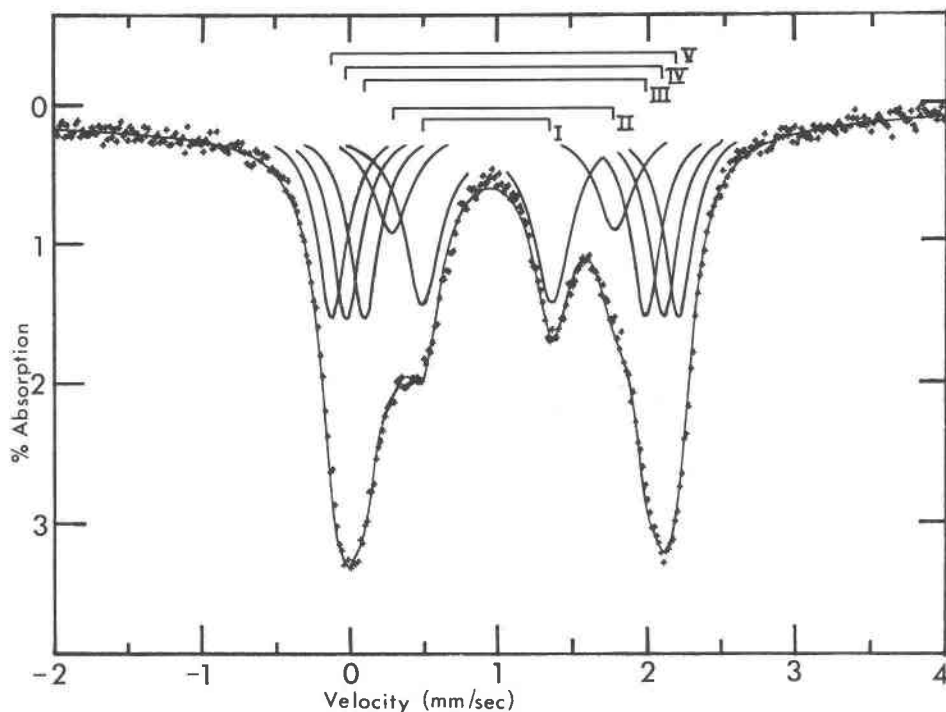


FIG. 3. The spectrum of sample A taken at 495 K showing individually the five doublets fitted to data.

The location of the ferrous ions giving the outer peaks in the spectra involves the majority of the iron in rhodonite. The width and asymmetry of each peak (as shown by the need to fit the peaks as three doublets) show several  $\text{Fe}^{2+}$  sites are involved in these absorptions. The finding of identical centers for the three doublets revealed that these peaks are symmetrical about a center point and indicated the various sites have a similar coordination. Thus, these peaks are assigned to  $\text{Fe}^{2+}$  in the three near octahedral sites  $M_1$ ,  $M_2$ , and  $M_3$ . The room temperature IS value of 1.21 mm/sec and QS values for the three doublets of 2.3, 2.5 and 2.7 mm/sec are typical of a  $\text{Fe}^{2+}$  coordination octahedra having some distortion (Bancroft, Maddock, and Burns, 1967; Greenwood and Gibbs, 1970). Attempts to assign a particular site to one of the fitted doublets are considered unjustifiable for several reasons. Firstly, the width of the lines of these doublets, while being either the same or slightly greater than the minimum observed with a thin iron absorber on the apparatus used, is narrower than generally observed for  $\text{Fe}^{2+}$  in silicate minerals (Bancroft, Maddock, and Burns, 1967; Law, 1973). The fit was thus suspected as being somewhat artificial. Secondly, the

three doublets were constrained to have equal intensities. Attempts to remove this constraint, by fixing the centers and peak widths of the three doublets the same and allowing the splitting and relative depths to vary, were tried with the best data sets. A small increase in  $\chi^2$  and larger standard deviations indicated the parameters were now interdependent. This model was, therefore, not pursued further.

A comparison of the three sites (Fig. 1) shows that each site has one elongated bond and one short bond, with  $M_3$  having the longest and  $M_2$  the shortest. The oxygen ions coordinated to the three sites will also differ in their effective charges.  $M_3$  has one oxygen ion coordinated to two Si ions, which should reduce the charge on that oxygen ion considerably. Both  $M_3$  and  $M_2$  have two C-type oxygen ions which have one less M bond than B type, and should carry the highest effective charge. Thus, considering both the various bond lengths and oxygen types, one may expect on the basis of distortion alone a QS correlation of  $M_3 < M_2 < M_1$ . However, while studies on wide ranges of minerals have shown (Bancroft, Maddock, and Burns, 1967; Greenwood and Gibbs, 1970) that in general there is a broad correlation of decreasing QS with increasing distortion of the ox-

TABLE 2. Parameters Derived from Fitting Five Doublets to the Rhodonite Spectra

		A			B		C		D	
		77K	295K	495K	77K	295K	77K	295K	77K	295K
I	IS*	1.189	1.076	0.963	1.187	1.078	1.192	1.086	1.194	1.09
	QS*	1.75	1.27	0.87	1.76	1.27	1.79	1.36	1.78	1.33
	$\Gamma^*$	0.32	0.35	0.30	0.30	0.33	0.32	0.34	0.30	0.32
II	IS	1.31	1.20	1.07	1.33	1.21	1.30	1.19	1.29	1.17
	QS	2.19	1.93	1.50	2.43	1.93	2.19	2.02	2.21	1.98
	$\Gamma^{**}$	0.35	0.37	0.31	0.51	0.35	0.25	0.46	0.29	0.36
	A†	0.18	0.45	0.62	0.37	0.47	0.14	0.60	0.28	0.61
III	IS	1.328	1.208	1.080	1.331	1.214	1.334	1.212	1.330	1.210
	QS	2.61	2.29	1.90	2.65	2.31	2.66	2.32	2.65	2.29
IV	IS	2.77	2.51	2.13	2.78	2.53	2.76	2.53	2.77	2.5
	QS	2.95	2.70	2.33	2.95	2.71	2.91	2.74	2.94	2.7
V	$\Gamma^*$	0.26	0.24	0.24	0.23	0.23	0.26	0.23	0.23	0.23
	A†	2.21	2.12	2.64	1.95	2.24	1.98	1.78	1.85	1.97
	$\chi^2$	292	665†	585†‡	275	232	245	243	240	240
	B $\epsilon$	1.86	1.85	4.55	1.61	2.41	4.41	7.79	3.82	8.16

\* Isomer shift (IS), quadruple splitting (QS) and full width at half height ( $\Gamma$ ) in mm/sec.

\*\*Estimated error in these values  $\pm 0.1$  mm, sec<sup>-1</sup>.

† Area (A) relative to area of innermost doublet = 1.0.

‡ 512 channel spectra.

$\epsilon$  Baseline/10<sup>4</sup>

xygen coordination polyhedra from octahedral symmetry, anomalous differences in QS between similar sites can occur. Consequently, in the absence of other evidence, correlations between QS and site geometry based on the site distortion alone can only be tentative.

The remaining doublet in the spectra, doublet II, can be assigned to Fe<sup>2+</sup> in the seven-coordinate site M<sub>5</sub>. The IS of these Fe<sup>2+</sup> ions is similar to the IS of the Fe<sup>2+</sup> ions in sixfold coordination but as the site is very distorted, the simple trend of increasing IS with coordination number is not expected to hold. Of more interest are the changes with temperature in the area of this doublet relative to that of the other four doublets.

In fitting the spectra the width and depth parameters of doublet III were found to have relatively large standard deviations. These deviations are attributed to small errors in the larger, neighboring peaks which have a large effect on this small doublet. The consequent uncertainty in the area of doublet II is difficult to measure but could be up to 50 percent. However, the four samples gave similar variations between 77 K and 295 K, and the spectrum at 495 K gave a convincing result that doublet II was increasing in area relative to the other absorptions.

These changes can be related to the large size of the M<sub>5</sub> site which is approximately 1.0 Å in radius, thus making it the preferred calcium site in rhodonite. The smaller Fe<sup>2+</sup> ions could move around in this site in the manner similar to that found for Fe<sup>2+</sup> ions in the 1.0 Å radius holes in thorium oxide (Shechter, Dash, Erickson, and Ingalls, 1970). The

Fe<sup>2+</sup> ions, in nominally eight-fold coordination, gave a low recoilless fraction which also had a much smaller temperature dependence than could be described by models assuming harmonic vibration of the Fe<sup>2+</sup> ions. The behavior of the Fe<sup>2+</sup> ions was explained by assuming them to be moving in a "wine bottle"-shaped potential well. This low temperature dependence of the recoilless fraction for a Fe<sup>2+</sup> ion in an over-large site could account for the area changes if the absorption from the Fe<sup>2+</sup> in the M<sub>5</sub> site decreases with temperature at a slower rate than that from the other sites. The difficulties in fitting the spectra make accurate measurements to confirm this behavior difficult, but the area changes appear to agree with the assignment of doublet II to the Fe<sup>2+</sup> ions in the M<sub>5</sub> site.

### (b) The Iron Distribution in Rhodonite

The inability to resolve clearly the spectra of Fe<sup>2+</sup> in the M<sub>1</sub>, M<sub>2</sub>, and M<sub>3</sub> sites makes quantitative comments on the iron distribution difficult. If the iron distribution among the three M<sub>1</sub>, M<sub>2</sub>, and M<sub>3</sub> sites is equal, then the relative areas from the spectra show the iron ions have some preference for the M<sub>4</sub> site. This is expected as Fe<sup>2+</sup> ions appear to prefer the more distorted sixfold coordination sites in other minerals such as cummingtonites (Bancroft, Burns, and Maddock, 1967) and orthopyroxenes (Bancroft, Burns, and Howie, 1967). It is difficult to determine if there would be any ordering of Fe<sup>2+</sup> amongst the M<sub>1</sub>, M<sub>2</sub>, and M<sub>3</sub> sites, and no evidence can be obtained from the spectra to suggest that there is or is not ordering. The M<sub>5</sub> site is clearly not a favored site for the ferrous ions.

Of more interest is the lack of any significant differences in the relative distribution of iron among the sites with changes in iron concentration. The spectra of samples A and D, in which the iron proportion of the total metal varies from 22.0 percent to 2.7 percent, can be fitted with almost identical parameters, whereas one would expect the absorption due to iron in a preferred site to increase relative to that of iron in a less preferred site. This is explained by applying Henry's Law to the solid solution of FeSiO<sub>3</sub> in (Mn,Ca)SiO<sub>3</sub>. As shown in Figure 4, the site populations can be approximated as linearly dependent on the FeSiO<sub>3</sub> concentration; hence no changes will be seen in the relative populations. Only with 25 percent to 75 percent FeSiO<sub>3</sub> in rhodonite would the relative populations significantly alter. Unfortunately, the maxi-

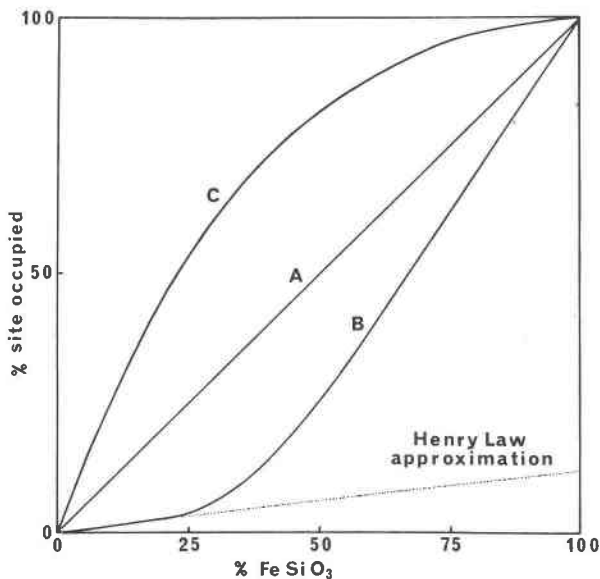


FIG. 4. Schematic diagram of the site population dependence on composition for the solid solution of  $\text{FeSiO}_3$  in  $(\text{Mn,Ca})\text{SiO}_3$ . Curve A would hold for sites with random cation distribution, curves B and C for sites showing preference for different cations. The almost linear dependence of site population on composition at low concentrations (Henry's Law) is apparent.

imum iron content of rhodonite is approximately 25 percent  $\text{FeSiO}_3$  (Deer, Howie, and Zussman, 1963); thus the relative site populations are unable to show if ordering has occurred.

### Conclusion

The Mössbauer spectra of four rhodonite samples show the ferrous iron to be distributed among the five possible cation sites. Most of the iron is in the 3 octahedral  $M_1$ ,  $M_2$ , and  $M_3$  sites, though the iron shows some preference for the  $M_4$  site. Site  $M_5$  has the lowest population. These results are contrary to those previously determined by X-ray methods (Peacor and Niizeki, 1963) and show that contributions from iron in all sites can be expected in optical spectra of rhodonite.

### Acknowledgments

The author would like to thank G. E. Halford for supplying the samples of Devon and Cornwall rhodonite, N. Ware for the electron microprobe analyses, and Dr. M. Marshall for several helpful discussions.

### References

BANCROFT, G. M., R. G. BURNS, AND R. A. HOWIE (1967) Determination of cation distribution in orthopyroxene by the Mössbauer effect. *Nature*, **213**, 1221–1223.

- \_\_\_\_\_, \_\_\_\_\_, AND A. G. MADDOCK (1967) Determination of cation distribution in the cummingtonite—grunerite series by Mössbauer spectra. *Am. Mineral.* **52**, 1009–1026.
- \_\_\_\_\_, \_\_\_\_\_, AND A. J. STONE (1968) Applications of the Mössbauer effect to silicate mineralogy—II. Iron silicates of unknown and complex structures. *Geochim. Cosmochim. Acta*, **32**, 547–559.
- \_\_\_\_\_, A. G. MADDOCK, AND R. G. BURNS (1967) Applications of the Mössbauer effect to silicate mineralogy—I. Iron silicates of known crystal structure. *Geochim. Cosmochim. Acta*, **31**, 2219–2246.
- CLARK, M. G., G. M. BANCROFT, AND A. J. STONE (1967) The Mössbauer spectrum of  $\text{Fe}^{2+}$  in a square planar environment. *J. Chem. Phys.* **47**, 4250–4261.
- DEER, W. A., R. A. HOWIE, AND J. ZUSSMAN (1963) *Rock-Forming Minerals*, Vol. II, *Chain Silicates*. Longman Group, Ltd., London.
- DOWTY, E., AND D. H. LINDSLEY (1973) Mössbauer spectra of synthetic hedenbergite—ferrosilite pyroxenes. *Am. Mineral.* **58**, 850–868.
- EVANS, M. J., AND P. J. BLACK (1970) The Voigt profile of Mössbauer transmission spectra. *J. Phys. C., Solid State Phys.* **3**, 2167–2177.
- GREENWOOD, N. N., AND T. C. GIBB (1971) *Mössbauer Spectroscopy*. Chapman and Hall, Ltd., London.
- INGALLS, R. (1964) Electric field gradient tensor in ferrous compounds. *Phys. Rev.* **133A**, 787–795.
- KEESTER, K. L., AND W. B. WHITE (1968) Crystal-field spectra and chemical bonding in manganese minerals. In P. Gay, A. F. Seager, H. F. W. Taylor, and J. Zussman, Eds., *Int. Mineral. Assoc. Pap. Proc. Fifth General Meet., Cambridge, 1966*. The Mineralogical Society, London, p. 22–35.
- LAKSHMAN, S. V. J., AND B. J. REDDY (1973) Optical absorption spectrum of  $\text{Mn}^{2+}$  in rhodonite. *Physica*, **66**, 601–610.
- LAW, A. D. (1973) Critical evaluation of statistical “best fits” to Mössbauer spectra. *Am. Mineral.* **58**, 128–131.
- MANNING, P. G. (1968) Absorption spectra of the manganese-bearing chain silicates pyroxmangite, rhodonite, bustamite, and serandite. *Can. Mineral.* **9**, 348–357.
- OVERTON, R. (1968) *A Study of Some Single Crystals of Rhodonite from Broken Hill, New South Wales*, B.Sc. (Hons.) Thesis, University of Sydney, N.S.W.
- PEACOR, D. R., AND N. NIIZEKI (1963) The redetermination and refinement of the crystal structure of rhodonite,  $(\text{Mn,Ca})\text{SiO}_3$ . *Z. Kristallogr.* **119**, 98–116.
- SHECHTER, H., J. G. DASH, G. A. ERICKSON, AND R. INGALLS (1970) Mössbauer study of low temperature aharmonicity in  $\text{ThO}_2:\text{Co}^{57}$ . *Phys. Rev. B*, **2**, 613–624.
- VIOLET, C. E., AND D. N. PIPCORN (1971) Mössbauer line positions and hyperfine interactions in  $\alpha$ -iron. *J. Appl. Phys.* **42**, 4339–4342.
- WINDOW, B., B. L. DICKSON, P. ROUTCLIFFE, AND K. K. P. SRIVASTAVA (1974) A versatile multiple Mössbauer spectrometer. *J. Phys. E.* (in press).